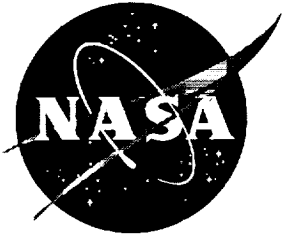


1N-24  
065089

NASA Contractor Report 201728



# Translaminar Fracture Toughness of a Composite Wing Skin Made of Stitched Warp-knit Fabric

*John E. Masters*

---

November 1997

## *The NASA STI Program Office ... in Profile*

Since its founding, NASA has been dedicated to the advancement of aeronautics and space science. The NASA Scientific and Technical Information (STI) Program Office plays a key part in helping NASA maintain this important role.

The NASA STI Program Office is operated by Langley Research Center, the lead center for NASA's scientific and technical information. The NASA STI Program Office provides access to the NASA STI Database, the largest collection of aeronautical and space science STI in the world. The Program Office is also NASA's institutional mechanism for disseminating the results of its research and development activities. These results are published by NASA in the NASA STI Report Series, which includes the following report types:

- **TECHNICAL PUBLICATION.** Reports of completed research or a major significant phase of research that present the results of NASA programs and include extensive data or theoretical analysis. Includes compilations of significant scientific and technical data and information deemed to be of continuing reference value. NASA counter-part of peer reviewed formal professional papers, but having less stringent limitations on manuscript length and extent of graphic presentations.
- **TECHNICAL MEMORANDUM.** Scientific and technical findings that are preliminary or of specialized interest, e.g., quick release reports, working papers, and bibliographies that contain minimal annotation. Does not contain extensive analysis.
- **CONTRACTOR REPORT.** Scientific and technical findings by NASA-sponsored contractors and grantees.

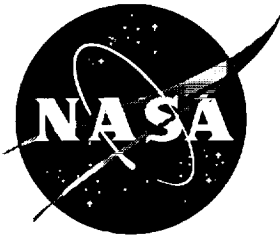
- **CONFERENCE PUBLICATION.** Collected papers from scientific and technical conferences, symposia, seminars, or other meetings sponsored or co-sponsored by NASA.
- **SPECIAL PUBLICATION.** Scientific, technical, or historical information from NASA programs, projects, and missions, often concerned with subjects having substantial public interest.
- **TECHNICAL TRANSLATION.** English-language translations of foreign scientific and technical material pertinent to NASA's mission.

Specialized services that help round out the STI Program Office's diverse offerings include creating custom thesauri, building customized databases, organizing and publishing research results ... even providing videos.

For more information about the NASA STI Program Office, see the following:

- Access the NASA STI Program Home Page at <http://www.sti.nasa.gov>
- E-mail your question via the Internet to [help@sti.nasa.gov](mailto:help@sti.nasa.gov)
- Fax your question to the NASA Access Help Desk at (301) 621-0134
- Phone the NASA Access Help Desk at (301) 621-0390
- Write to:  
NASA Access Help Desk  
NASA Center for Aerospace Information  
800 Elkridge Landing Road  
Linthicum Heights, MD 21090-2934

NASA Contractor Report 201728



# Translaminar Fracture Toughness of a Composite Wing Skin Made of Stitched Warp-knit Fabric

*John E. Masters*

*Lockheed Martin Engineering and Sciences, Hampton, Virginia*

National Aeronautics and  
Space Administration

Langley Research Center  
Hampton, Virginia 23681-2199

Prepared for Langley Research Center  
under Contract NAS1-96014

---

November 1997

The use of trademarks or names of manufacturers in the report is for accurate reporting and does not constitute an official endorsement, either expressed or implied, of such products or manufacturers by the National Aeronautics and Space Administration.

---

Available from the following:

NASA Center for AeroSpace Information (CASI)  
800 Elkridge Landing Road  
Linthicum Heights, MD 21090-2934  
(301) 621-0390

National Technical Information Service (NTIS)  
5285 Port Royal Road  
Springfield, VA 22161-2171  
(703) 487-4650

## **Abstract:**

A series of tests were conducted to measure the fracture toughness of carbon/epoxy composites. The composites were made from warp-knit carbon fabric and infiltrated with epoxy using a resin-film-infusion process. The fabric, which was designed by McDonnell Douglas for the skin of an all-composite subsonic transport wing, contained fibers in the 0°, ±45°, and 90° directions. Layers of fabric were stacked and stitched together with DuPont Kevlar® yarn to form a 3-dimensional preform.

Three types of test specimens were evaluated: compact tension, center notch tension, and edge notch tension. The effects of specimen size and crack length on fracture toughness were measured for each specimen type.

These data provide information on the effectiveness of the test methods and on general trends in the material response. The scope of the investigation was limited by the material that was available.

## **Introduction**

McDonnell Douglas will design and build an all-composite wing for a commercial transport aircraft as part of NASA's AST Composite Wing Program. The design will address the requirements of the FAA's FAR Airworthiness Standards. This includes the requirement that the wing maintain adequate strength after sustaining detectable impact damage and discrete source damage. Traditionally, discrete source damage is represented as a two-bay crack. A fracture mechanics methodology is being developed by NASA to address this requirement and to support the wing design.

This report describes the results of a program conducted to develop experimental data in support of NASA's analytical efforts. A series of tests were conducted to measure the fracture toughness of composites made of stitched warp-knit fabric. Three test methods were investigated: compact tension, center notch tension, and edge notch tension. Tests were conducted to assess the sensitivity of the test results to specimen size, crack length, and specimen thickness. Notch opening displacement was also monitored in some tests to define the onset of damage at the notch tips and to establish failure mechanisms.

A description of the materials tested is provided in the next section. This will be followed by a definition of the test specimens and experimental procedures. A review of the test results is given in the following section. The final section of the report provides a few summary observations.

## **Materials Investigated.**

The composites tested in this study were fabricated from an AS4 carbon warp-knit fabric made using technologies adapted from the textile industry. The fabric, which was designed by McDonnell Douglas for the skin of an all-composite subsonic transport wing, contained AS4 fibers in the 0°, ±45°, and 90° directions. The orientation and areal weight of each ply of fibers in the fabric is listed in Table I. By

---

Kevlar is a registered trademark of E. I. DuPont.

areal weight, 44% of the fibers were configured in the 0° direction, 44% in the ±45° directions, and 12% in the 90° direction. Layers of fabric were stacked and stitched together using a modified lock stitch to form a 3-dimensional preform of required thickness. Kevlar 29 yarns of 1600 and 400 denier were used for the needle and bobbin threads, respectively. The thickness of the stitched warp-knit fabric is 0.056 inches per layer, which is equivalent to 54 plies of prepreg with a 4.3oz/yd<sup>2</sup> areal density. The same fabric was stitched together to make tee-shaped stiffeners that were also stitched to the skin. After stitching, the preforms were infiltrated with 3501-6 epoxy using a resin-film-infusion process.

Table I. Preform Fiber Orientation and Areal Weight

Ply Number	Orientation	Fiber Areal Weight (oz/yd <sup>2</sup> )
1	+45	5.19
2	-45	5.19
3	0	10.9
4	90	5.86
5	0	10.9
6	-45	5.19
7	+45	5.19

All the specimens tested in this study were fabricated using the materials and procedures described above. They differed only in their thickness and stitch spacing. Test specimens were obtained from two sources. Most were machined from a large structural test panel that had been fabricated by McDonnell Douglas in Long Beach, CA and tested at NASA Langley. This 5-stringer panel featured blade stiffeners spaced 8 inches apart. Test specimens were cut from the undamaged sections of wing skin material between the stiffeners. The remaining specimens were machined from two plain 35-inch by 44-inch plates fabricated at NASA Langley.

### McDonnell Douglas Material

The specimens machined from the 5-stringer panel consisted of six layers of the warp-knit fabric. The fabric was stitched (8 stitches/inch) in the 0° fiber direction. The rows of stitches were 0.5 inches apart.

The target fiber volume content was 54.2%. On average, the actual fiber volume content, which was determined through the matrix digestion technique defined in ASTM Test Method D-3171 was 55.4%. An examination of the specimens indicated that over-compaction of the stitched fabric during manufacture resulted in a 0.025-inch-thick layer of neat resin on one surface of the composites. Discounting this surface layer, the composites had an effective fiber volume content of 59.4%. Stresses were calculated using the thickness associated with the 55.4% fiber volume content.

A series of tensile tests were conducted to determine unnotched tensile properties. The modulus, Poisson's ratio, and strength were measured. These properties were measured in the axial or 0° direction only. The transverse properties

could not be measured since a viable transverse tension specimen could not be made from the material between the panel's stiffeners. The results of these tests are summarized in Table II.

Table II. Warp-knit Material's Axial Tensile Properties (6 fabric layers)

Specimen No.	Modulus, Msi	Poisson's Ratio	Max. Stress, ksi
501-T1	10.5	0.398	117.2
501-T2	10.3	0.406	122.0
501-T3	10.8	0.408	118.5
501-T4	10.1	0.384	118.6
Avg. ± Std.Dev.	10.4 ± 0.30	0.399 ± 0.011	119.2 ± 2.1

### NASA Langley Material

The test panels fabricated at NASA Langley consisted of only two layers of the warp-knit fabric. The thickness of the test specimens machined from these panels were, therefore, 1/3 that of specimens cut from the 5-stringer panel fabricated by McDonnell Douglas. Like the Douglas material, these panels were also stitched in the 0° fiber direction at a stitch density of 8 stitches/inches. However, the rows of stitches were only 0.2 inches apart.

The mechanical properties of these panels were determined by Dr. Alan T. Nettles of the Mechanics of Materials Branch at NASA Langley Research Center. A summary of the tensile properties measured are contained in Table III.

Table III. Warp-knit Material's Axial Tensile Properties (2 fabric layers)

Property	Longitudinal, Avg. ± Std.Dev.	Transverse, Avg. ± Std.Dev.
Modulus, Msi	10.19 ± 0.19	4.05 ± 0.06
Poisson's Ratio	0.400 ± 0.058	0.172 ± 0.009
Max. Stress, ksi	131.1 ± 7.0	40.4 ± 2.6

A comparison of the data in the two tables indicates that the two materials had comparable axial properties. Dr. Nettles' data also provides a measure of the material's anisotropy.

Poe (Ref. 1) derived the following expression to compute the fracture toughness of a composite laminate in terms of constituent properties and a characteristic distance  $d_0$  equal to 0.30 inches<sup>1/2</sup>, which was evaluated using test data.

$$(K_I)_{pred} = \epsilon_{tuf} \sqrt{2\pi d_0} E_x \left(1 - \sqrt{\nu_{xy} \nu_{yx}}\right)^{-1}$$

The  $0^\circ$  layers are assumed to be the critical layers, and the fibers and matrix are assumed to be well bonded. Representing the stitched warp-knit fabric as a laminate and taking the tensile failing strain of the fibers as  $\epsilon_{\text{tuf}} = 0.0148$  and the elastic constants as  $E_x = 10.4$  Msi,  $E_y = 5.22$  Msi,  $\nu_{xy} = 0.403$ ,  $\nu_{yx} = 0.202$ , the above equation gives the fracture toughness  $(K_I)_{\text{pred}} = 64.5 \text{ ksi}\cdot\text{inches}^{1/2}$ . Also, for the composite rotated  $90^\circ$  relative to the crack, the equation with the subscripts x and y interchanged gives the fracture toughness  $(K_I)_{\text{pred}} = 32.4 \text{ ksi}\cdot\text{inches}^{1/2}$ . Notice that the term  $\nu_{xy}\nu_{yx}$  is the same for both composite orientations and that  $(K_I)_{\text{pred}}$  is therefore proportional to the elastic modulus perpendicular to the crack.

## Test Specimens and Experimental Procedures.

Three test methods were used to measure the material's fracture toughness: compact tension, center notch tension, and edge notch tension. The specimen sizes were varied in each type of test to determine if test results were sensitive to specimen geometry. The ratio of the notch length, a, to the specimen width, W, was also varied in these tests to measure the sensitivity of the toughness measurements to this parameter.

### Compact Tension Test Specimens

The Compact Tension Test Specimens evaluated in this investigation were based on the specimen design defined in ASTM test method E-399-90. That method was developed to measure the plane-strain fracture toughness of metallic materials. Two specimen sizes were tested. Their geometries are defined in Figures 1 and 2. As the figures indicate, the Large Compact Tension Specimens are twice the size of the Small Compact Tension Specimens.

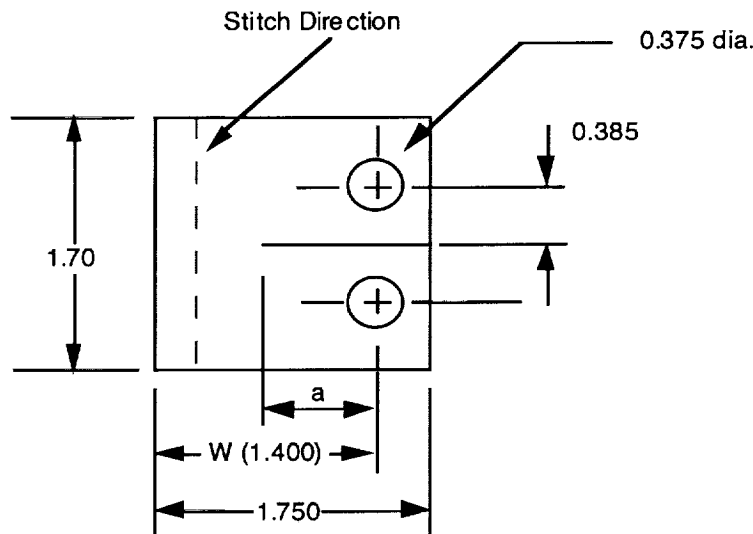


Figure 1. Small Compact Tension Geometry.



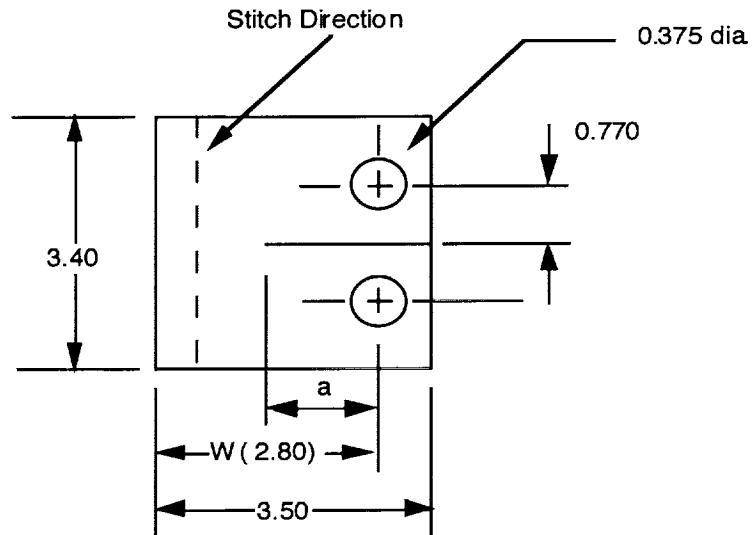


Figure 2. Large Compact Tension Specimen Geometry.

Compact Tension tests were conducted at a range of  $a/W$  ratios. The Small Compact Tension Specimens had nominal  $a/W$  ratios of 0.45, 0.50, and 0.55. The Large Compact Tension Specimens were to be tested at the same ratios. However, due to an error in the specimen drawings, these specimens featured nominal  $a/W$  ratios of 0.60, 0.65, and 0.70.

Table IV gives the test matrix for the compact tension tests. As the table indicates, fracture toughness was measured for crack growth in the direction perpendicular to the  $0^\circ$  fibers in most cases. One set of Large Compact Tension specimens were fabricated with the notch parallel to the  $0^\circ$  fibers to measure fracture toughness for crack growth in this direction.

The critical dimensions of all the compact tension specimens tested are given in Table V.

Table IV. Number of Compact Tension Tests.

Notch Orientation	Nominal $a/W$ Ratio					
	0.45	0.50	0.55	0.60	0.65	0.70
Small Specimen (1.7 inches x 1.75 inches)						
Notch $\perp$ to $0^\circ$ Fibers	1	2	2	-	-	-
Large Specimen (3.4 inches x 3.5 inches)						
Notch $\perp$ to $0^\circ$ Fibers	-	-	-	1	1	1
Notch $\parallel$ to $0^\circ$ Fibers	-	-	-	1	1	1

Table V. Compact Tension Specimen Dimensions.

Specimen Number	Thickness, inches	Width, inches	Actual a/W Ratio
Small Specimens (1.7 inches x 1.75 inches) with Notch $\perp$ to $0^\circ$ Fibers			
501-CT-11	0.354	1.409	0.46
501-CT-21	0.351	1.407	0.50
501-CT-22	0.353	1.409	0.51
501-CT-31	0.352	1.403	0.56
501-CT-32	0.352	1.404	0.56
Large Specimens (3.4 inches x 3.5 inches) with Notch $\perp$ to $0^\circ$ Fibers			
CT-1L	0.330	2.759	0.57
CT-2L	0.331	2.825	0.63
CT-3L	0.331	2.800	0.69
Large Specimens (3.4 inches x 3.5 inches) with Notch $\parallel$ to $0^\circ$ Fibers			
CT-1L90	0.326	2.809	0.57
CT-2L90	0.325	2.809	0.63
CT-3L90	0.326	2.809	0.69

### Center Notch Tension Test Specimens

Three center notch tension test specimens were evaluated in this study. They have been identified by their widths - 2-Inch-Wide, 4-Inch-Wide, and 12-Inch-Wide Specimens.

The 2- and 4-Inch-Wide Center Notch Specimens, shown in Figures 3 and 4, respectively, were fabricated from material taken from the structural test panel material described earlier. They featured six layers of the warp-knit fabric. As the figures demonstrate, the 4-Inch-Wide Specimens were twice as long and wide as the 2-Inch-Wide Specimens. Two crack length/specimen width ( $2a/W$ ) ratios, 0.25 and 0.33, were evaluated for each specimen type.

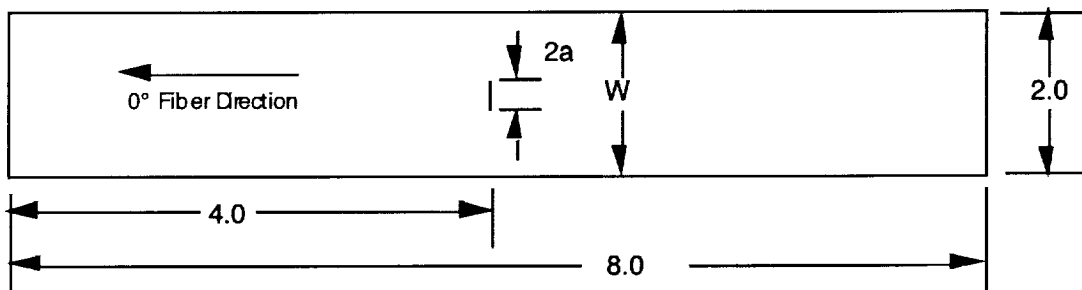


Figure 3. 2-Inch-Wide Center Notch Tension Specimen Geometry.

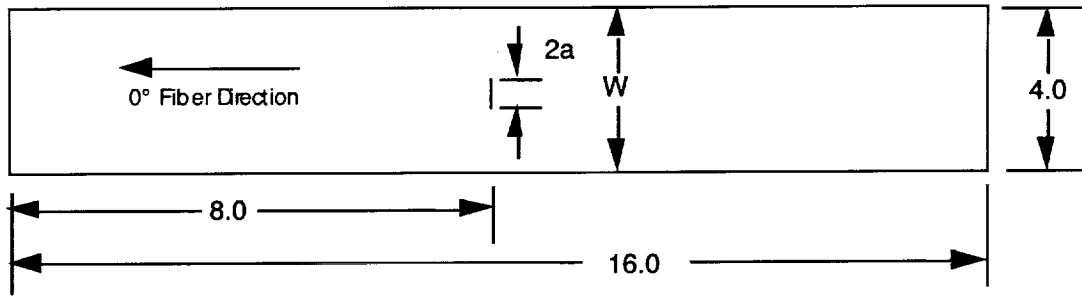


Figure 4. 4-Inch-Wide Center Notch Tension Specimen Geometry.

The 12-Inch-Wide Center Notch Tension Specimens are shown in Figure 5. They were fabricated at NASA Langley using two layers of the warp-knit fabric defined in Table III. The notch length was varied over a wider range in these specimens to determine whether R-Curve effects were present when the thinner material was tested. Five specimens were tested; their notch lengths ranged from 3.0 inches to 5.0 inches. The  $2a/W$  ratios evaluated ranged from 0.25 to 0.42.

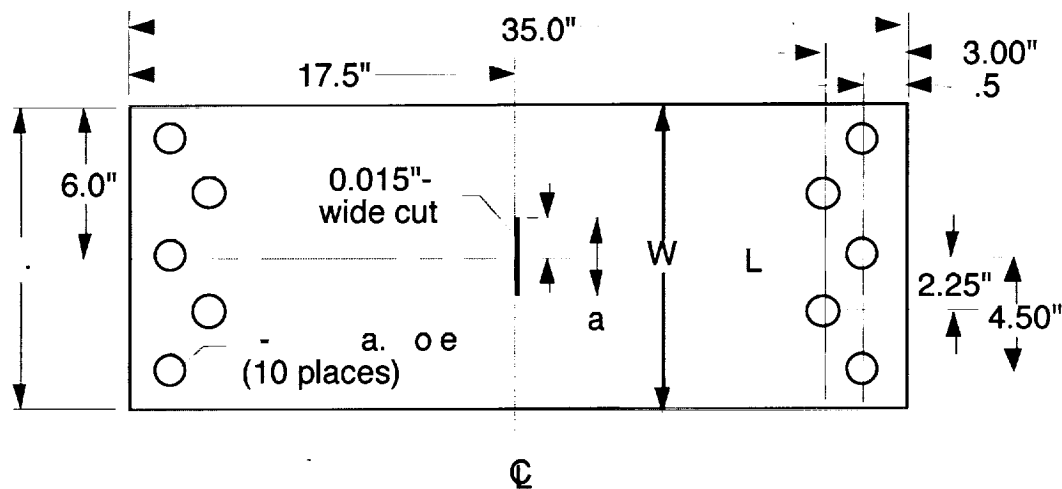


Figure 5. 12-Inch-Wide Center Notch Tension Specimen.

In addition to the three specimens described above, a series of Inclined Center Notch Tension specimens with notches inclined at  $45^\circ$  to the loading direction were also fabricated and tested. They were tested to provide a measure of the effect of mixed Mode I and Mode II loading on fracture toughness. Their projected notch length/specimen width ratios ( $2a'/W$ ) were comparable to the 2-Inch-Wide Specimen's  $2a/W$  ratios. These specimens are shown in Figure 6.

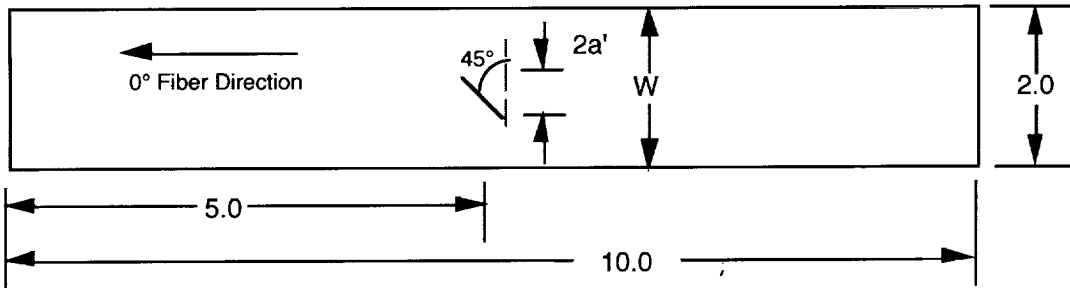


Figure 6. Inclined Center Notch Tension Specimen.

The 2- and 4-Inch-Wide and Inclined Center Notch Specimens were tested in load frames equipped with hydraulic grips. The 2- and 4-Inch-Wide Center Notch Specimens had a test section length to width ratio of 2.0. The Inclined Center Notch Specimens had a slightly longer test section length to accommodate the inclined notch. They had a test section length/width ratio of 2.5. Bolted mechanical grips were used to test the 12-Inch-Wide specimens. They also had a test section length/width ratio of 2.0.

Table VI gives the test matrix for the center notch tension tests. With the exception of the Inclined Center Notch Specimens, all notches were oriented perpendicular to the 0° fiber direction. Center notch specimens were not tested for crack growth parallel to the 0° fibers.

Table VI. Number of Center Notch Tension Tests.

Specimen Type	Nominal $2a/W$ Ratio				
	0.25	0.29	0.33	0.375	0.42
2-Inch-Wide Specimen	1	-	1	-	-
<sup>1</sup> Inclined Notch Specimen	1	-	1	-	-
4-Inch-Wide Specimen	1	-	1	-	-
12-Inch-Wide Specimen	1	1	1	1	1

<sup>1</sup>Ratio of projected notch length to specimen width,  $2a'/W$ .

The critical dimensions of all the Center Notch Tension specimens tested are given in Table VII.

Table VII. Center Notch Tension Specimen Dimensions.

Specimen Number	Thickness, Inches	Width, inches	Actual 2a/W Ratio
2-Inch-Wide Specimens (2.0 inches x 8.0 inches)			
501-CN2	0.343	2.001	0.26
501-CN3	0.346	2.002	0.34
Inclined Notch Specimens (2.0 inches x 8.0 inches)			
501-ICN1	0.323	2.01	0.25*
501-ICN2	0.324	2.02	0.33*
4-Inch-Wide Specimens (4.0 inches x 16.0 inches)			
501-CN1L	0.326	4.003	0.25
501-CN2L	0.325	4.000	0.34
12-Inch-Wide Specimens (12.0 inches x 35.0 inches)			
2A#1	0.113	12.005	0.42
2B#2	0.113	11.995	0.38
2A#2	0.113	12.005	0.33
2B#3	0.112	12.015	0.29
2A#3	0.112	11.910	0.25

\* Ratio of Projected Notch Length to specimen width, 2a/W.

### Edge Notch Tension Test Specimens

Two edge notch tension specimens were also evaluated. Specimen size was again altered to determine if notch length effects were manifest. The specimens tested are shown in Figures 7 and 8.

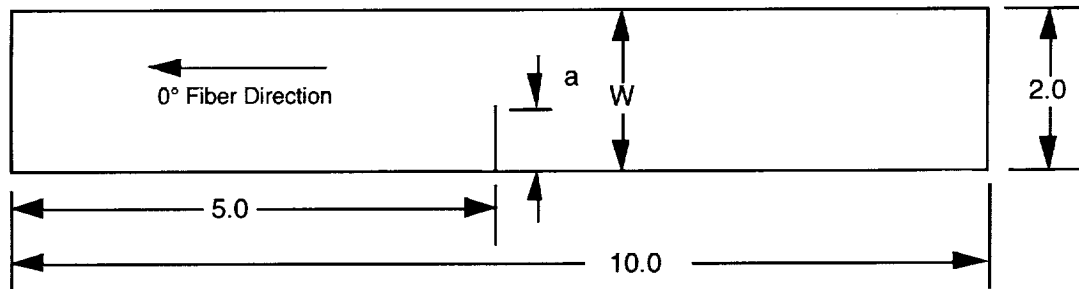


Figure 7. 2-Inch-Wide Edge Notch Tension Specimen Geometry.

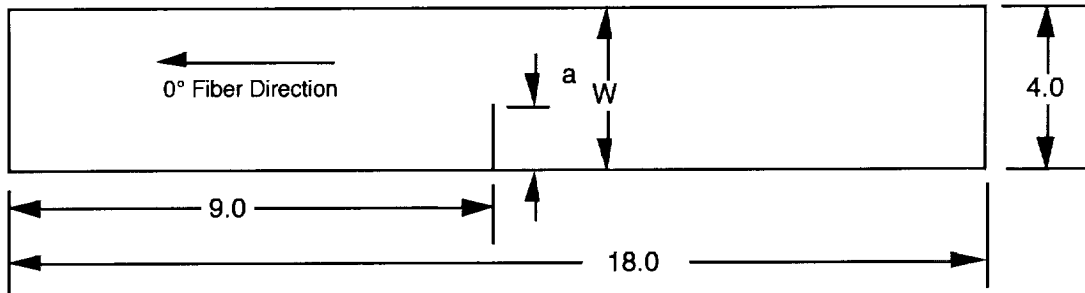


Figure 8. 4-Inch-Wide Edge Notch Tension Specimen Geometry.

Like the 2- and 4-Inch-Wide Center Notch specimens, the ends of the Edge Notch Specimens were also clamped during loading. Both the 2- and 4-Inch-Wide Edge Notch specimens had a test section length/width ratio of 3.0.

Table VIII gives the test matrix for the Edge Notch Tension Tests. All notches were oriented perpendicular to the 0° fiber direction. Edge notch specimens were not tested for crack growth parallel to the 0° fibers. The critical dimensions of all the Edge Notch Tension specimens tested are given in Table IX.

Table VIII. Number of Edge Notch Tension Tests.

Specimen Type	Nominal a/W Ratio		
	0.25	0.33	0.50
2-Inch-Wide Specimen	1	1	1
4-Inch-Wide Specimen	1	1	-

Table IX. Edge Notch Tension Specimen Dimensions.

Specimen Number	Thickness, Inches	Width, Inches	Actual a/W Ratio
2-Inch-Wide Specimens (2.0 inches x 8.0 inches)			
501-ENT1L	0.322	2.02	0.25
501-ENT2L	0.321	2.02	0.33
501-ENT3L	0.319	2.02	0.50
4-Inch-Wide Specimens (4.0 inches x 16.0 inches)			
501-EN1G	0.346	4.003	0.25
501-EN2G	0.338	4.004	0.34

### Experimental Procedures.

All fracture toughness tests conducted in this investigation were run in displacement control. A ramp rate of 0.05 inches/minute was employed in every test.

The load, cross head displacement, and crack opening displacement (COD) was monitored in all tests. These parameters were scanned and recorded once a

second. In addition, strain gages were mounted on a number of specimens to measure the far-field strains. Files of these data are available for analysis.

## Experimental Results.

### Compact Tension Test Results

The results of the compact tension tests are summarized in Table X. Two loads are listed in the table for each test. The values, listed as  $P_Q$ , were determined by applying the procedure defined in Section 9 of ASTM Test Method E399. This procedure is illustrated in Figure 9 where load is plotted against COD for the Small Compact Tension Specimen 501-CT-21. Section 9 instructs the investigator to draw a secant line through the origin of the test record with the slope  $(P/v)_5 = 0.95 (P/v)_0$ , where  $(P/v)_0$  is the slope of the tangent to the initial linear part of the record. The criteria listed in the test method define  $P_Q$  as the intercept of the  $(P/v)_5$  line and the load-COD curve since the load at every point on the record which precedes the intercept was lower than intercept value.

As Figure 9 illustrates, the specimen was able to sustain additional load beyond  $P_Q$ , however. This was the case in virtually all of the compact tension tests conducted. The maximum loads attained in each test are also listed in Table X. When this occurs, E399 requires the investigator to calculate the ratio of  $P_{max}/P_Q$ . If this ratio exceeds 1.10, the test is not considered a valid measure of plane strain fracture toughness,  $K_{IC}$ . The  $P_{max}/P_Q$  ratios calculated for each test are listed in the table. The data indicate that the values exceeded 1.10 in a majority of cases.

In interpreting these results, it should be noted that E399 was written for isotropic metallic specimens. Composite materials, are generally orthotropic and less homogeneous than metals. The applicability of fracture mechanics, in general, and this method, in particular, have yet to be established. The data presented in this report will contribute to that evaluation.

For an infinite plate containing a crack, the stress intensity factors for isotropic and orthotropic plates are equal (Ref. 2). Based on analytical work of Bowie and Freese (Ref. 3) for finite, orthotropic plates with a central crack, the isotropic equations for stress intensity factors are within 15% of orthotropic results. Similar accuracy is expected for the other specimens tested.

The fracture toughness was computed for each test using the following equation for isotropic materials given in E399.

$$K_I = (P / BW^{1/2}) f(a / W)$$

where:

$$f(a / W) = \frac{(2 + a / W)}{(1 - a / W)^{3/2}} \left( \begin{array}{l} 0.886 + 4.64a / W - 13.32a^2 / W^2 + 14.72a^3 / W^3 \\ -5.6a^4 / W^4 \end{array} \right)$$

where:

B = specimen thickness, inches

P = load, kips  
 W = specimen width, inches  
 a = notch length, inches  
 $f(a/W)$  = correction factor to account for specimen width effects

Both the maximum load,  $P_{max}$ , and the load determined by the offset method,  $P_Q$ , were substituted into this equation. The results are listed in the Table X.

Table X. Compact Tension Test Results.

Specimen Number	$P_Q$ , kips	$P_{max}$ , kips	$P_{max}/P_Q$	$f(a/W)$	$K_Q$ , ksi-in. <sup>1/2</sup>	$(K)_{max}$ , ksi-in. <sup>1/2</sup>	$(K)_{pred}$ , ksi-in. <sup>1/2</sup>
Small Specimens (1.7 inches x 1.75 inches) with Notch $\perp$ to 0° Fibers							
501-CT-11	2.49	2.68	1.08	8.58	50.8	54.7	64.5
501-CT-21	1.90	2.31	1.22	9.66	44.1	53.6	64.5
501-CT-22	1.63	2.32	1.42	9.96	38.7	55.1	64.5
501-CT-31	1.09	1.88	1.72	11.77	30.8	53.1	64.5
501-CT-32	1.41	1.90	1.35	11.77	39.8	53.6	64.5
Avg. $K_{max} \pm$ Std.Dev. = 54.0 $\pm$ 0.84							
Large Specimens (3.4 inches x 3.5 inches) with Notch $\perp$ to 0° Fibers							
CT-1L	2.68	2.78	1.04	12.20	59.6	61.9	64.5
CT-2L	2.30	2.60	1.13	15.44	63.8	72.2	64.5
CT-3L	1.47	1.88	1.28	20.45	54.3	69.4	64.5
Avg. $K_{max} \pm$ Std.Dev. = 67.8 $\pm$ 5.3							
Large Specimens (3.4 inches x 3.5 inches) with Notch $\parallel$ to 0° Fibers							
CT-1L90	1.62	1.68	1.04	12.20	36.2	37.5	32.4
CT-2L90	1.24	1.24	1.00	15.44	35.1	35.1	32.4
CT-3L90	0.80	0.91	1.14	20.45	30.1	34.1	32.4
Avg. $K_{m \times} \pm$ Std.Dev. = 35.6 $\pm$ 1.7							



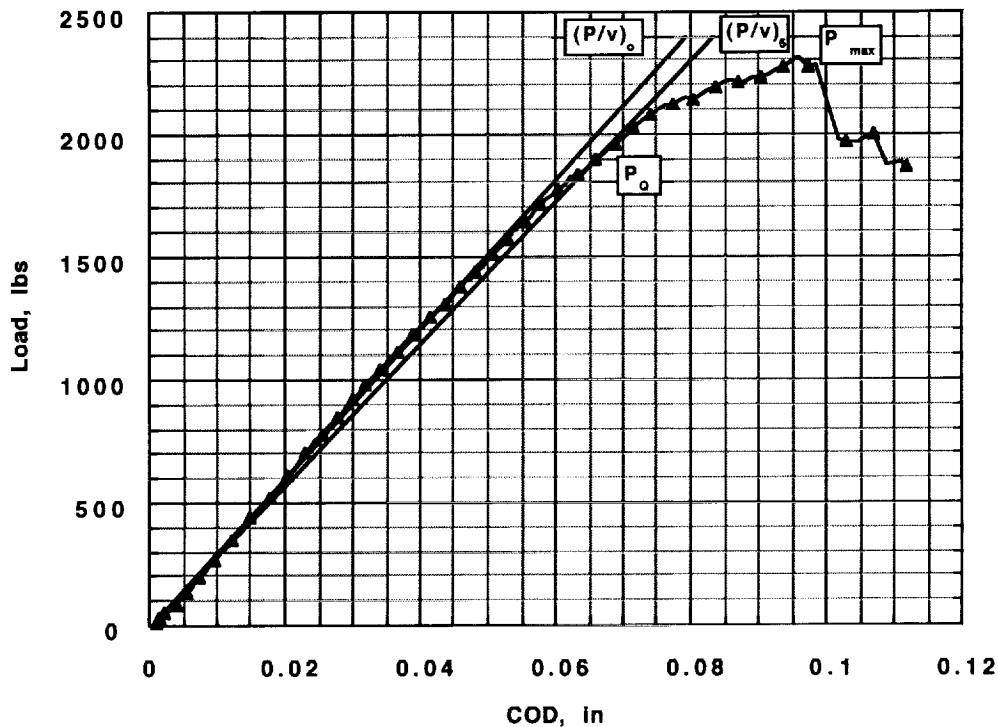


Figure 9. Load vs. COD for Small Compact Tension Specimen 501-CT-21.

Figure 10 plots the typical load vs. COD curve for Large Compact Tension Specimen CT-2L. As in the case of the Small Compact Tension Specimens, the notch was cut perpendicular to the  $0^\circ$  direction in this specimen.

A comparison of the results obtained for the Small specimen (Figure 9) and the Large specimen (Figure 10) indicates that, despite their size differences, the two specimens exhibited similar responses. The curves exhibit a nonlinear response prior the first load drop. Both specimens also continued to accept load beyond their  $P_0$  levels. Finally, they both reached a maximum load greater than 1.10 times the  $P_0$  value.

Although it is not reflected in these figures, the Large and Small Compact Tension Specimens failed in different manners. Macroscopic crack growth in the Small specimens was parallel to the  $0^\circ$  fibers. Failure progressed from the notch tip in a vertical direction. Failure in the Large specimens progressed in a horizontal direction from the notch tip, which is usually referred to as self-similar fracture. The non-self-similar fracture is sometimes observed in specimens that have positive T-stresses. (The stress intensity factor is the coefficient of the singular term in the Williams series expansion of stresses, and the T-stress is the coefficient of the zero order term.)

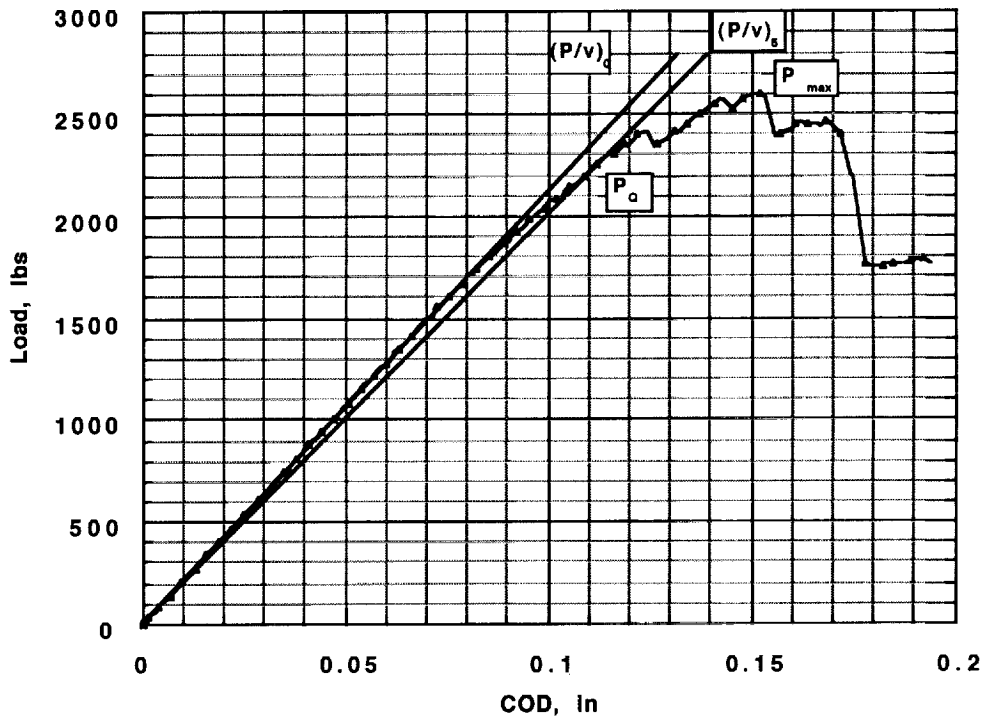


Figure 10. Load vs. COD for Large Compact Tension Specimen CT-2L.

Figure 11 plots the response of Specimen CT-2L90. This is a Large Compact Tension Specimen in which the notch was machined parallel to the  $0^\circ$  direction. These specimens also failed in a self-similar manner.

The figure illustrates that, as in the case of Specimen CT-2L (Figure 10), this specimen was also able to sustain additional load beyond  $P_0$ . However, in contrast to the specimens in which the crack growth was perpendicular to the  $0^\circ$  fibers, the maximum load sustained by the specimen was approximately equal to the load defined as  $P_0$ . As the data in Table X illustrates, this was the case in two of the three CT-L90 specimens tested.

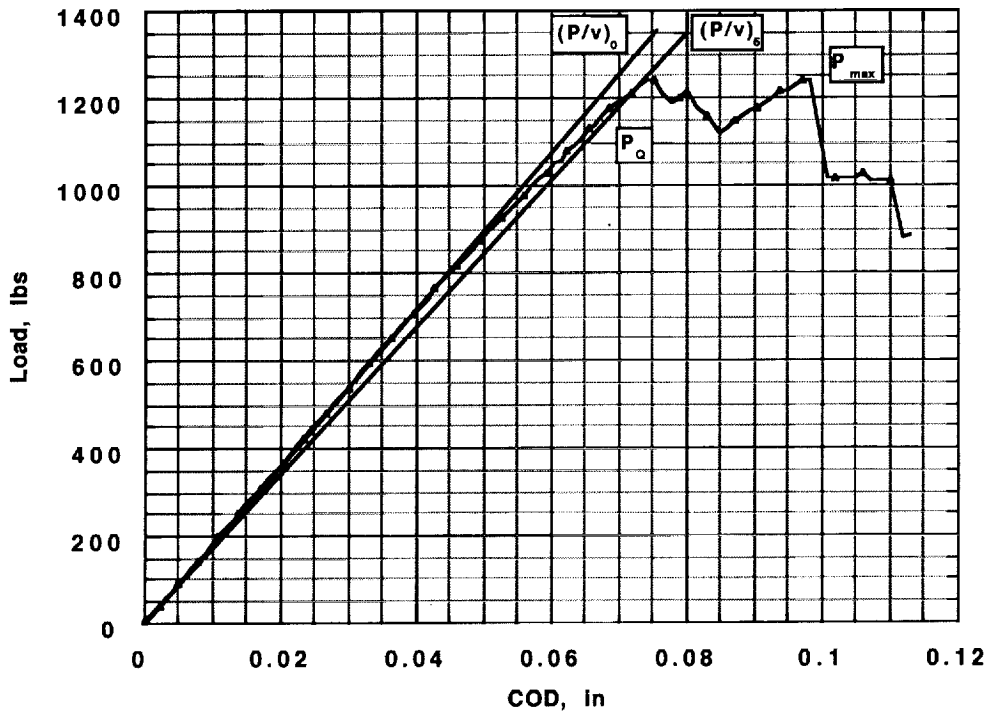


Figure 11. Load vs. COD for Large Compact Tension Specimen CT-2L90.

The values of  $(K_I)_{max}$  for the large compact specimens in Table X were 5 to 10% greater than the  $(K_I)_{pred}$  values, depending on notch orientation. Thus, the measured values were in reasonably good agreement with the predicted values. The values of  $(K_I)_{max}$  for the small compact specimens, which did not fail in a self-similar manner, were 84% of  $(K_I)_{pred}$ .

### Center Notch Tension Test Specimens

The results of the center notch tension tests are summarized in Table XI. The table lists the  $2a/W$  ratios plus the maximum loads attained during loading. The maximum stress values were computed by dividing the measured maximum loads by the cross-sectional areas which were computed using the dimensions given in Table VII.

Table XI. Center Notch Tension Test Results.

Specimen Number	Actual 2a/W Ratio	Max. Load, kips	Max. Stress, ksi	(K <sub>I</sub> ) <sub>max</sub> <sup>1</sup> , ksi-Inches <sup>1/2</sup>	(K <sub>I</sub> ) <sub>pred</sub> <sup>1</sup> , ksi-Inches <sup>1/2</sup>
2-Inch-Wide Specimens (2.0 inches x 8.0 inches)					
501-CN2	0.26	44.3	64.5	60.9	64.5
501-CN3	0.34	37.2	53.7	59.8	64.5
Inclined Notch Specimens (2.0 inches x 8.0 inches)					
501-ICN1	0.25 <sup>1</sup>	39.8	61.3	57.8	64.5
501-ICN2	0.33 <sup>1</sup>	37.7	57.6	62.4	64.5
4-Inch-Wide Specimens (4.0 inches x 16.0 inches)					
501-CN1L	0.25	76.7	58.8	77.2	64.5
501-CN2L	0.34	59.1	45.5	71.3	64.5
12-Inch-Wide Specimens (12.0 inches x 35.0 inches)					
2A#1 <sup>2</sup>	0.42	39.9	29.4	92.9	64.5
2B#2	0.38	52.6	38.8	113.5	64.5
2A#2	0.33	47.8	35.2	95.2	64.5
2B#3	0.29	57.7	42.9	106.6	64.5
2A#3	0.25	64.3	48.2	108.9	64.5

<sup>1</sup>Ratio of Projected Notch Length to specimen width, 2a/W.

<sup>2</sup>Specimen 2A#1 exhibited transverse buckling prior to failure. An anti-buckling guide was used to suppress buckling on all subsequent tests.

Except for the inclined notch specimens, the fracture toughness values listed in Table XI were computed using the following equation developed by Fedderson for isotropic materials (Ref. 2).

$$K_I = \sigma_{\infty} \sqrt{\pi a} [\sec(\pi a / W)]^{1/2}$$

where:

$\sigma_{\infty}$  = maximum applied stress

a = half crack length

W = specimen width

For the inclined notch specimens, the fracture toughness values were computed using the following equation for an infinitely wide specimen made of isotropic material (Ref. 4 with correction of Ref. 5).

$$K_I = \sigma_{\infty} \sqrt{\pi a} \left\{ \begin{aligned} & \sin(\beta) \cos\left(\frac{\theta}{2}\right) \left[ \sin(\beta) \cos^2\left(\frac{\theta}{2}\right) - \frac{3}{2} \cos(\beta) \sin(\theta) \right] \\ & + \sqrt{\frac{2c}{a}} [\cos^2(\beta) - \sin^2(\beta)] \sin^2(\theta) \end{aligned} \right\}$$

and

$$0 = \sin^2(\beta) \sin(\theta) - \sin(\beta) \cos(\beta) [1 - 3 \cos(\theta)] - \frac{16}{3} \sqrt{\frac{2c}{a}} [\cos^2(\beta) - \sin^2(\beta)] \sin\left(\frac{\theta}{2}\right) \cos(\theta)$$

where:

$a$  = half length of inclined crack.

$\beta$  = angle of inclination measured from direction of loading.

$\theta$  = direction of maximum polar stress  $\sigma_{\theta\theta}$  at a distance  $r = c$ . The angle  $\theta$  is measured from the inclined crack and has values between  $-90^\circ$  and  $0^\circ$ .

The antisymmetry of the inclined crack induces both Mode I and Mode II deformation at the notch tip. The presence of a Mode II component has been shown to cause the crack to turn from the direction of the inclined notch and follow a direction perpendicular to the applied load in a manner that maximizes the component of polar normal stress  $\sigma_{\theta\theta}$ . See for example Ref. 4. For  $\beta = 45^\circ$ , the direction  $\theta$  is equal to  $-53.13^\circ$ , independent of the distance  $c$ , and  $K_I = 0.8944\sigma_\infty\sqrt{\pi a} = 1.064\sigma_\infty\sqrt{\pi a}$ . Thus, the fracture is predicted to propagate initially  $98.13^\circ$  from the loading direction. Examination of the failed specimens revealed that the mean path of the fracture was about  $90^\circ$ . Matrix cracking in the surface  $45^\circ$  plies obscured the exact initial direction.

The average values of fracture toughness for the 2-Inch-Wide and Inclined Specimens were 6.7% less than the predicted value in Table XI. The fracture toughness values of the Inclined Specimens would be even closer if finite width correction factors were applied. The average values for the 4-Inch-Wide Specimens were 15% greater than the predicted value. Thus, the fracture toughness values for the 6-layer-thick material were reasonably close to the predicted value. On the other hand, the average fracture toughness value for the 12-Inch-Wide Specimens, which were made from the 2-layer-thick material, was 60% greater than the predicted value.

Poe (Ref. 1) has noted that thick and thin fracture specimens demonstrate different responses. A thin specimen's response may be dominated by a dispersed pattern of matrix cracking and delamination found in the specimen's outer layers. Although these failure mechanisms are present in the outer layers of thicker specimens, the specimen response in these cases is dominated by the constrained core of inner layers. Poe noted that damage in these inner layers is limited to a narrow band and that a well-defined crack surface is evident in these layers.

Figures 12 and 13 plot the COD vs. the applied stress for the Small and Large Center Notch Tension Specimens. Straight lines have been fit to the initial portions of the curves to aid in identifying the onset of damage development.

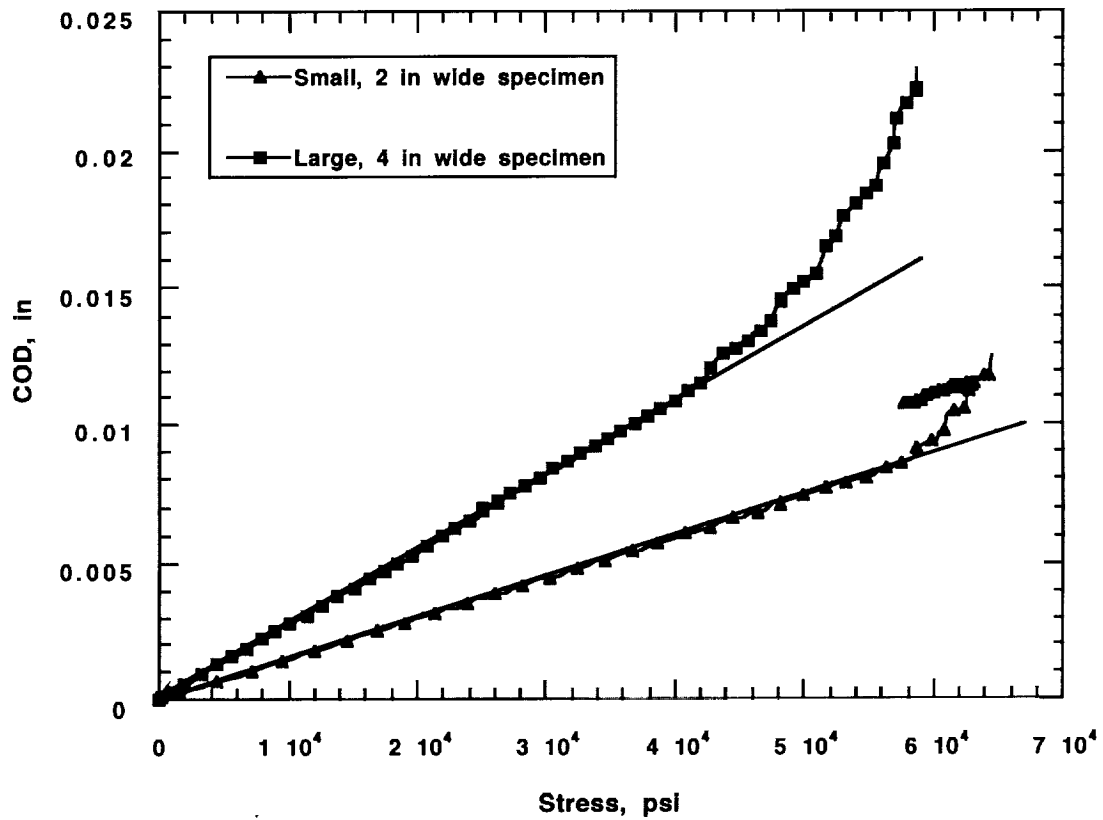


Figure 12. COD vs. Stress for Center Notch Specimens ( $2a/W = 0.25$ ).

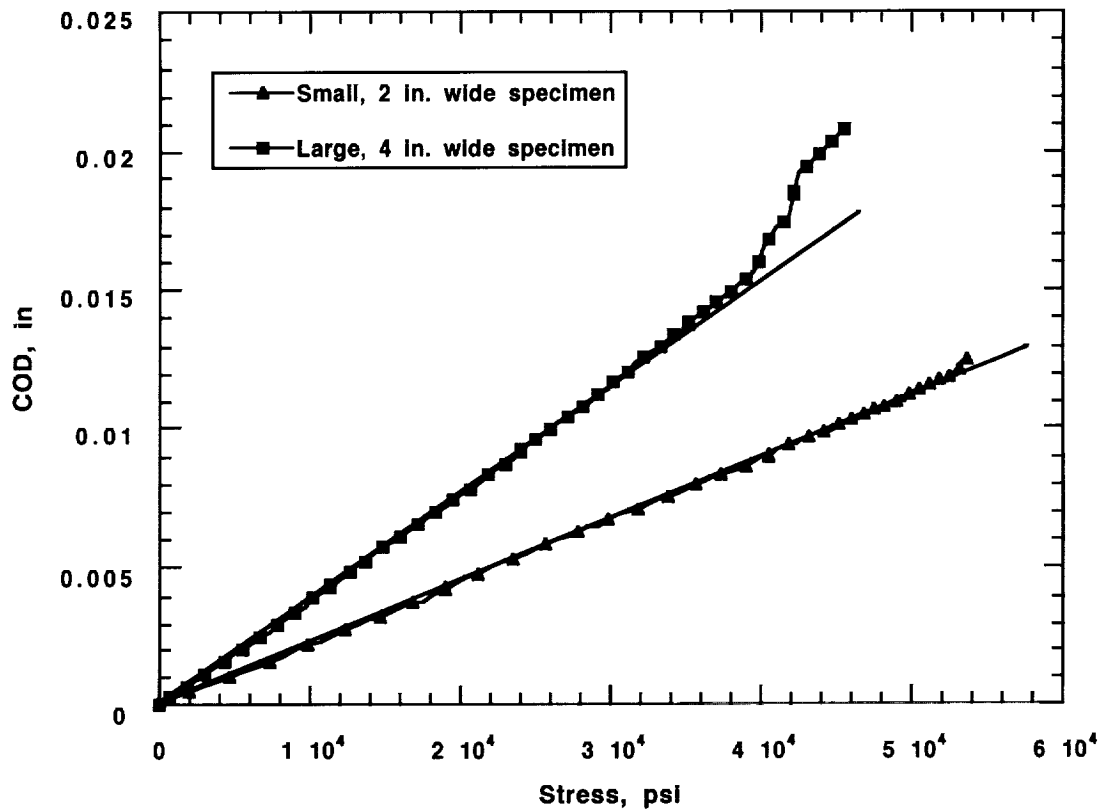


Figure. 13. COD vs. Stress for Center Notch Specimens ( $2a/W = 0.33$ ).

The COD vs. Load plot for a typical 12-Inch-Wide Specimen is shown in Figure 14. The specimen was loaded and unloaded four times prior to failure so that radiographs could be made of the damage at the crack tips. Test results indicated that large changes in the curves' slopes accompanied bursts of matrix cracking and delamination. This is seen during the fourth and final loading in this specimen.

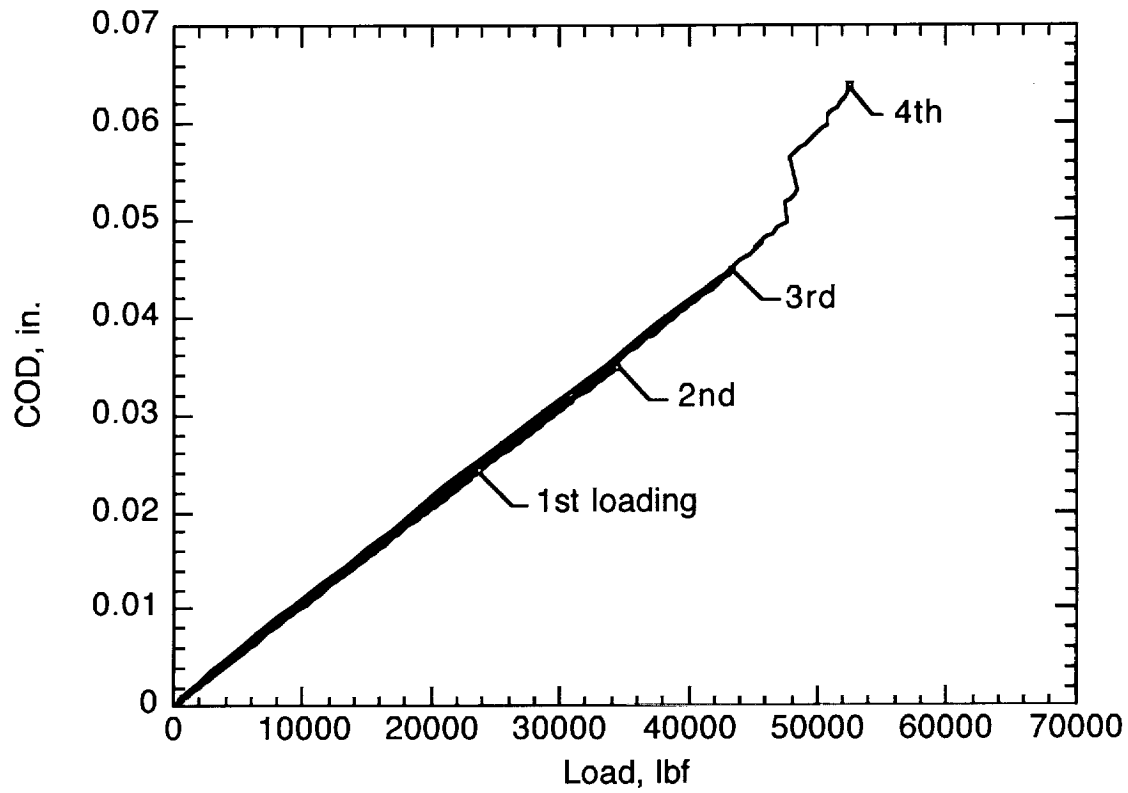


Figure 14. COD vs. Load for 12-Inch-Wide Center Notch Tension Specimen 2B#2.

### Edge Notch Tension Test Specimens

The results of the edge notch tension tests are summarized in Table XII. The table lists the  $a/W$  ratios plus the maximum loads attained during loading. As in the case of the center notch tension tests, the maximum stress values were computed by dividing the measured maximum loads by the cross-sectional areas which were computed using the specimen dimensions. These values are given in Table VIII.

The fracture toughness values listed in Table XII were computed using an equation developed by Gross (Ref. 2) for isotropic materials with uniform applied stress boundary conditions. The equation is given below:

$$K_I = \sigma_\infty \sqrt{\pi a} \left[ 1.12 - 0.23(a/W) + 10.6(a/W)^2 - 21.7(a/W)^3 + 30.4(a/W)^4 \right]$$

where:

- $\sigma_\infty$  = maximum applied stress
- $a$  = crack length
- $W$  = specimen width

The values of  $K_I$  in Table XII are 41 to 108% greater than  $K_{I, \text{pred}}$ . It should be noted, however, that the boundary conditions that existed in these tests were more



nearly uniform applied displacement. Bloom (Ref. 6) has shown that stress intensity factors under uniform displacement conditions can be much smaller than those for uniform stress conditions, depending on specimen configuration. Thus, the values of  $K_I$  are probably calculated incorrectly.

Table XII. Edge Notch Tension Test Results.

Specimen Number	Actual a/W Ratio	Max. Load, kips	Max. Stress, ksi	$(K_I)_{max}$ , ksi-inches <sup>1/2</sup>	$(K_I)_{pred}$ , ksi-inches <sup>1/2</sup>
Small Specimens (2.0 inches x 8.0 inches)					
501-ENT1L	0.25	31.6	48.6	91.2	64.5
501-ENT2L	0.33	25.3	39.0	101.1	64.5
501-ENT3L	0.50	16.9	26.2	134.2	64.5
Large Specimens (4.0 inches x 16.0 inches)					
501-EN1G	0.25	51.3	37.0	99.7	64.5
501-EN2G	0.34	40.1	29.6	112.5	64.5

Figures 15 and 16 plot the crack opening displacement (COD) vs. net stress curves for the Small and Large Edge Notch Tension tests. The data measured for specimens with a nominal a/W ratio of 0.25 are shown in Figure 15. The 0.33 a/W data are shown in Figure 16. Straight lines have again been fit to the initial portions of the curves to aid in identifying the onset of damage development.

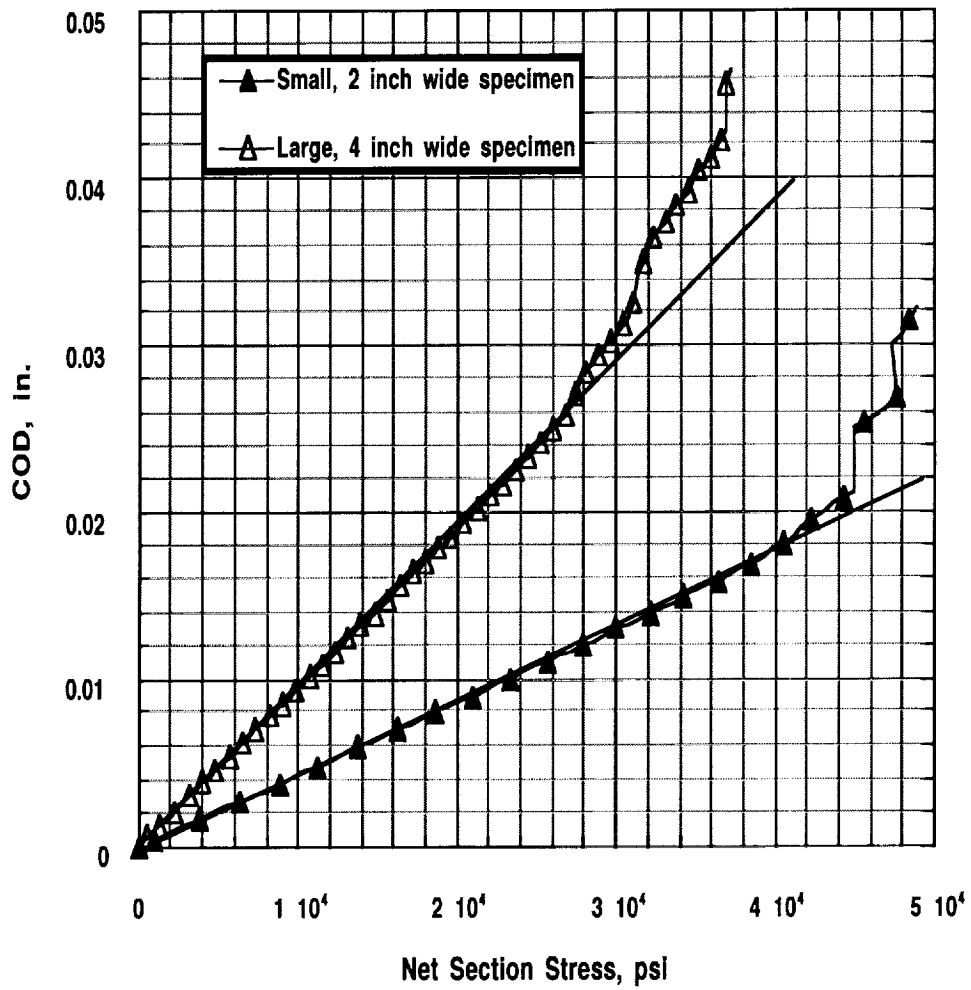


Figure 15. COD vs. Stress for Edge Notch Specimens ( $a/W = 0.25$ ).

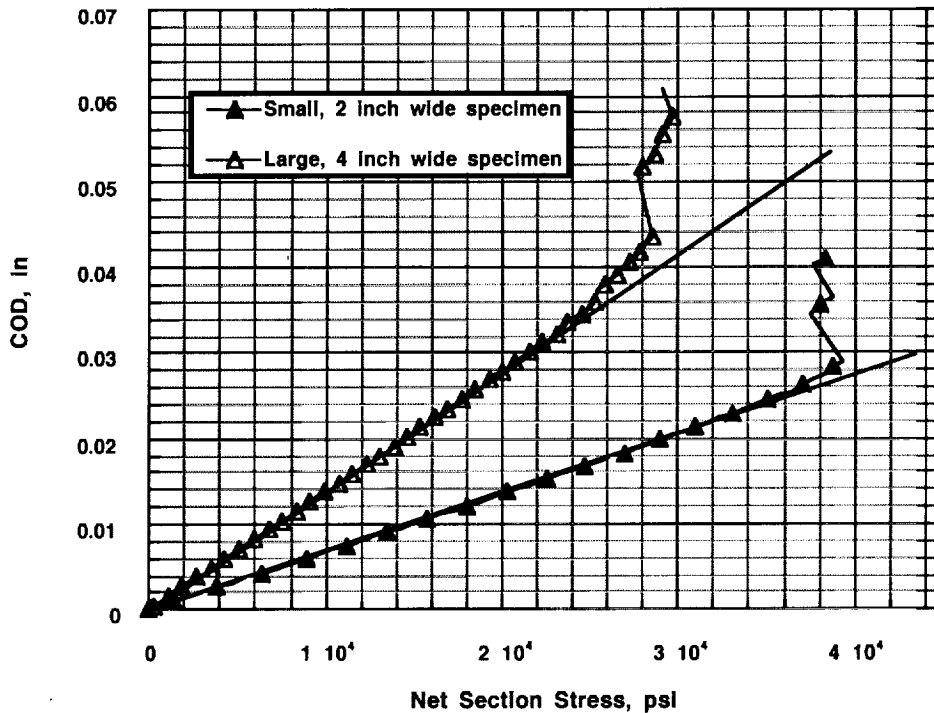


Figure 16. COD vs. Stress for Edge Notch Specimens ( $a/W = 0.33$ ).

## Summary

A series of exploratory tests were conducted to determine the fracture toughness of stitched multi-axial warp-knit material. Compact tension, center notch tension, and edge notch tension specimens were evaluated. Empirical data were developed to establish the effects of specimen thickness, notch size, and specimen size on the material response. Values of fracture toughness were also predicted from constituent properties for comparison.

These data provide information on the effectiveness of the test methods and on general trends in the material response. The limited amount of material available limited the scope of the investigation.

The results of the tests are summarized below by test type. Fracture toughness values are also summarized in Figure 17 for all test types.

### Compact Tension Tests

- The values of fracture toughness for the large compact specimens were within 10% of the predicted values.
- The values of fracture toughness for notches oriented parallel to the  $0^\circ$  fibers were about one half the values for notches oriented perpendicular to the  $0^\circ$  fibers. As predicted, the values of fracture toughness increased in proportion to the elastic modulus in the direction of loading.

- The  $P_{max}/P_Q$  ratios exceeded 1.10 in a majority of cases indicating that the fracture toughness values measured were invalid using the criteria listed in ASTM E399. It should be noted, however, that this criteria was developed for isotropic metals.
- The Large and Small Specimens exhibited distinctly different macroscopic failures. The cracks grew in a self-similar fashion in the Large Specimens but grew perpendicular to the notch in the Small Specimens. The values of fracture toughness for the Small Specimens were 84% of the predicted value.

### **Center Notch Tension Tests**

- The average values of fracture toughness for the 2- and 4-Inch-Wide Specimens and Inclined Specimens were between -6.7% and 15% of the predicted value.
- The average value of fracture toughness for the 12-Inch-Wide Specimens was 60% greater than the predicted value. The 12-Inch-Wide Specimens were much thinner than the other specimens. The small thickness is believed to cause the high toughness since the thick and thin composites had similar unnotched mechanical properties.
- The crack grew approximately perpendicular to the applied load in the Inclined Notch Specimens as predicted.

### **Edge Notch Tension Tests**

- The values of fracture toughness were 41 to 108% greater than the predicted value. This discrepancy is probably due to the assumption of uniform stress. The actual boundary condition was more nearly uniform displacements. Numerical results in the literature indicate that the stress intensity factor would be significantly lower for uniform displacements than for uniform stress.

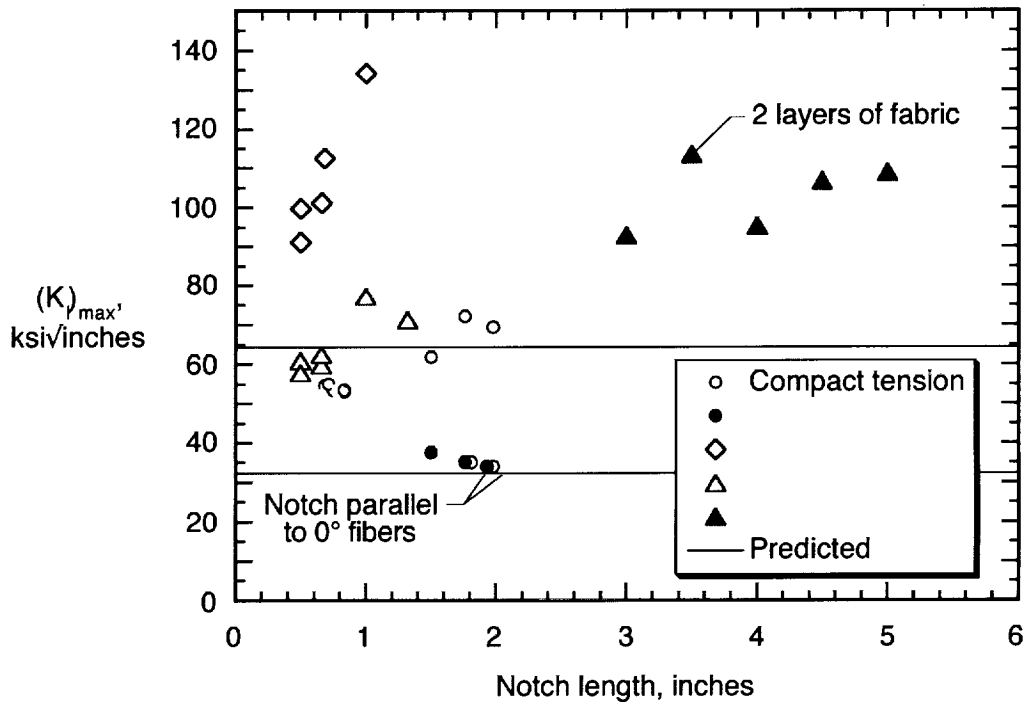


Figure 17. Summary of Fracture Toughness Values for all test types.

## References

1. Poe, Jr. C. C., "Residual Strength of Composite Aircraft Structures with Damage," ASM Handbook, Vol. 19, Fatigue and Fracture, 1996, pp. 920-935.
2. Tada, H., "The Stress Analysis of Cracks Handbook," Second Edition, Paris Productions Incorporated, 226 Woodbourne Dr. St. Louis, MO, 63105, 1985.
3. Bowie, O. L. and Freese, C. E., "Central Crack in Plane Orthotropic Rectangular Sheet," Int. Jour. Fract. Mech., Vol. 8, No. 1, March 1972, pp. 49-58.
4. Williams, J. G. and Ewing, P. D., "Fracture under Complex Stress - The Angled Crack Problem," Int. Jour. Fract. Mech., Vol. 8, No. 4, December 1972, pp. 441-446.
5. Finnie, I. and Saith, A., "A Note on the Angled Crack Problem and the Directional Stability of Cracks," Int. Jour. of Fracture, 9, 1973, pp. 484-486.
6. Bloom, Joseph M., "The Short Single Edge Crack Specimen with Linearly Varying End Displacements," Int. Jour. Fract. Mech., Vol. 2, No. 4, December 1996, pp. 597-603.

REPORT DOCUMENTATION PAGE			Form Approved OMB No. 0704-0188	
Public reporting burden for this collection of information is estimated to average 1 hour per response, including the time for reviewing instructions, searching existing data sources, gathering and maintaining the data needed, and completing and reviewing the collection of information. Send comments regarding this burden estimate or any other aspect of this collection of information, including suggestions for reducing this burden, to Washington Headquarters Services, Directorate for Information Operations and Reports, 1215 Jefferson Davis Highway, Suite 1204, Arlington, VA 22202-4302, and to the Office of Management and Budget, Paperwork Reduction Project (704-0188), Washington, DC 20503.				
1. AGENCY USE ONLY (Leave blank)		2. REPORT DATE November 1997	3. REPORT TYPE AND DATES COVERED Contractor Report	
4. TITLE AND SUBTITLE Translaminar Fracture Toughness of a Composite Wing Skin Made of Stitched Warp-knit Fabric			5. FUNDING NUMBERS NAS1-96014 WU 538-10-11-05	
6. AUTHOR(S) John E. Masters				
7. PERFORMING ORGANIZATION NAME(S) AND ADDRESS(ES) Lockheed Martin Engineering and Sciences Hampton, VA 23681-0001			8. PERFORMING ORGANIZATION REPORT NUMBER	
9. SPONSORING/MONITORING AGENCY NAME(S) AND ADDRESS(ES) National Aeronautics and Space Administration Langley Research Center Hampton, VA 23681-2199			10. SPONSORING/MONITORING AGENCY REPORT NUMBER NASA CR-201728	
11. SUPPLEMENTARY NOTES Langley Technical Monitor: C. C. Poe, Jr. Final Report - Task DM25				
12a. DISTRIBUTION/AVAILABILITY STATEMENT Unclassified-Unlimited Subject Category 24 Distribution: Nonstandard Availability: NASA CASI (301) 621-0390			12b. DISTRIBUTION CODE	
13. ABSTRACT (Maximum 200 words) A series of tests were conducted to measure the fracture toughness of carbon/epoxy composites. The composites were made from warp-knit carbon fabric and infiltrated with epoxy using a resin-film-infusion process. The fabric, which was designed by McDonnell Douglas for the skin of an all-composite subsonic transport wing, contained fibers in the 0°, ±45°, and 90° directions. Layers of fabric were stacked and stitched together with Kevlar yarn to form a 3-dimensional preform.  Three types of test specimens were evaluated: compact tension, center notch tension, and edge notch tension. The effects of specimen size and crack length on fracture toughness were measured for each specimen type.  These data provide information on the effectiveness of the test methods and on general trends in the material response. The scope of the investigation was limited by the material that was available.				
14. SUBJECT TERMS Fracture toughness; Fracture tests; Textile composites; warp-knit fabric; stitching; Resin film infusion, AS4 carbon fiber; 3501-6 epoxy resin			15. NUMBER OF PAGES 30	
			16. PRICE CODE A03	
17. SECURITY CLASSIFICATION OF REPORT Unclassified	18. SECURITY CLASSIFICATION OF THIS PAGE Unclassified	19. SECURITY CLASSIFICATION OF ABSTRACT Unclassified	20. LIMITATION OF ABSTRACT	